

Acoustic anomaly in the antiferrodistortive phase transition of KHCO_3 studied by Brillouin scattering

S. Takasaka, Y. Tsujimi, and T. Yagi

Research Institute for Electronic Science, Hokkaido University, Sapporo 060, Japan

(Received 28 April 1997)

Brillouin-scattering spectra of KHCO_3 have been observed as a function of temperature. The two pure transverse acoustic modes propagating along the a^* and b axes show an anomalous softening near the phase-transition temperature $T_N=318$ K. Their frequencies, however, are nonzero even at T_N . This incomplete softening behavior indicates an antiferrodistortive phase transition, though a ferroelastic transition was suggested by a previous ultrasonic study. A phenomenological discussion is given for the antiferrodistortive phase transition. [S0163-1829(97)03541-8]

Potassium hydrogen carbonate, KHCO_3 , undergoes a structural phase transition at $T_N=318$ K.¹ Recently, Kashida and Yamamoto studied the crystal structure by x-ray analysis.² The structure is characterized by the orientational configuration of a planar $(\text{HCO}_3)_2$ dimer. In the high-temperature phase (phase I), each dimer is in a disordered configuration as shown in Fig. 1(a). The space group of the crystal is monoclinic $C2/m$. In the low-temperature phase (phase II), dimers are ordered in an antiphase configuration as shown in Fig. 1(b). The space group is monoclinic $P2_1/a$.²⁻⁴ In phase II, the dimer takes one of two orientations as shown in Fig. 1(b). The change of the crystal structure strongly suggests that KHCO_3 undergoes an antiferrodistortive phase transition of the order-disorder type.

On the other hand, Haussühl performed an ultrasonic experiment and concluded that the phase transition of KHCO_3 is of ferroelastic type. This conclusion is based on the experimental fact that the elastic stiffness constant c_{66} , related to the pure transverse acoustic modes propagating along the a^* and b axes, shows an anomalous softening near T_N .¹ In the case of the ferroelastic transition, however, the spontaneous shear strain x_{6s} appears with the freezing of any of these acoustic modes; that is, the frequency of such a soft mode should take a zero value at the transition point. In addition to this, the crystal structure should be triclinic $P\bar{1}$ in phase II with the appearance of x_{6s} . This crystal structure $P\bar{1}$ is inconsistent with the result of x-ray studies $P2_1/a$.²⁻⁴

The purpose of the present paper is to solve this inconsistency. All the acoustic modes propagating along the a^* , b , and c axes were reexamined by a 90° Brillouin scattering system in the temperature range between 295 and 355 K. In particular, the anomalous behaviors of the pure transverse acoustic modes propagating along the a^* and b axes were carefully investigated near T_N to elucidate whether the frequencies of these modes take zero values at T_N or not. The present paper is a report of the Brillouin scattering of a KHCO_3 crystal.

A single crystal of KHCO_3 was grown from an aqueous solution by slow cooling. The crystal axes were confirmed by x-ray diffraction pattern analysis and also by the observation of the crystal habit. The rectangular prism shaped sample, $5 \times 5 \times 8$ mm³, was obtained on referring to the

dominant cleavage plane $(40\bar{1})$ and the natural rectangular plane (100) . After the surfaces of the sample was polished up, the sample was mounted in a light scattering cell. The temperature of the sample was measured by a thermocouple placed near the sample and was controlled within ± 0.05 K. A longitudinal single-mode Ar^+ laser (Spectra-Physics, BeamLok 2060) was used as a light source. The wavelength and the output power of the laser beam were 514.5 nm and 80 mW, respectively. The scattered light from the sample was collected in the 90° Brillouin scattering geometry. A three-passed tandem Sandercock-type Fabry-Pérot interferometer was used as a spectrometer. The free spectral ranges employed here were 10 and 30 GHz. The finesse was maintained at more than 100 throughout the present experiment. The analyzed light was detected by a photomultiplier

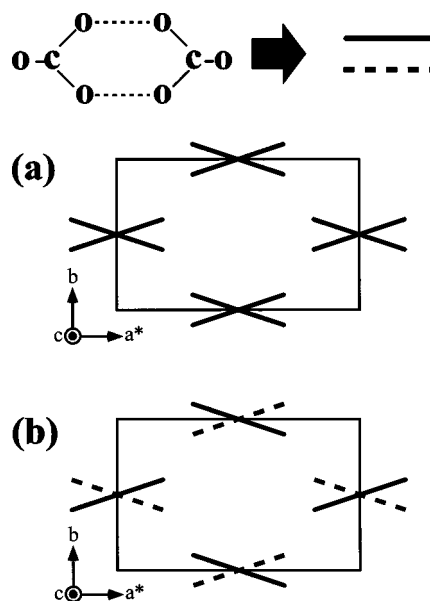


FIG. 1. The configuration of $(\text{HCO}_3)_2$ dimers on the c -axis projection. A dimer containing two hydrogen bonds ($\text{O} \cdots \text{O}$) is represented by a solid line or a dashed line. A unit cell is designated by a rectangle. (a) In the high-temperature phase (phase I), each dimer takes a disordered configuration. (b) In the low-temperature phase (phase II), dimers are ordered in one of two antiphase configurations expressed by a solid and dashed lines.

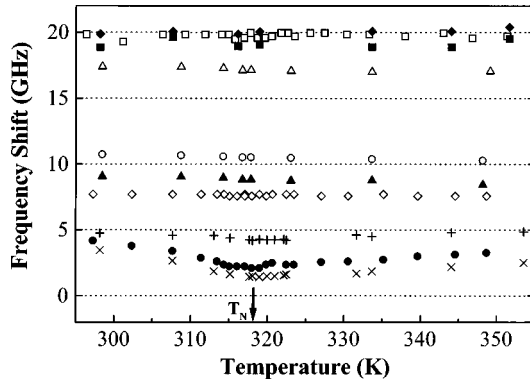


FIG. 2. The temperature dependence of the frequency shifts of the quasi- c_{11} (\square), the quasi- c_{55} (\diamond), and the c_{66} (\bullet) modes propagating along the a^* axis; the c_{22} (\blacklozenge), the quasi- c_{44} (\blacksquare), and the c_{22}''' (\times) modes propagating along the b axis; the quasi- c_{33} (\triangle), the c_{44} (\circ), and the quasi- c_{55} (\blacktriangle) modes propagating along the c axis. The evaluated frequency $F(c_{46})$ ($+$) is also shown.

(Hamamatsu R585) and was accumulated in the memory of a multichannel analyzer. From the Brillouin scattering spectra obtained after 1200 time repetitions of accumulation, the frequency shift of the Brillouin peak was evaluated by the fit of the damped harmonic oscillator function.

All nine acoustic modes propagating along the a^* , b , and c axes are observed precisely near T_N by 90° Brillouin scattering. The frequency shift of each mode is plotted in Fig. 2 as a function of temperature. Two modes show remarkable softening behavior near T_N . One is the pure c_{66} mode propagating along the a^* axis and the other is the pure transverse acoustic mode, named the c_{22}''' mode in Ref. 1, propagating along the b axis. The typical spectra of these modes, which are measured with a high-frequency resolution of 0.1 GHz, are depicted in Figs. 3(a) and 3(b). The frequency shift data of these modes are plotted again in Fig. 4 on an expanded scale. Both of the c_{66} and the c_{22}''' modes soften toward T_N as reported by Haussühl (Ref. 1). In addition to this fact, we found that their frequencies do not take zero values even at T_N : 2.1 GHz for the c_{66} mode and 1.4 GHz for the c_{22}''' mode. This incomplete softening behavior strongly indicates that the phase transition mechanism of KHCO_3 is not of ferroelastic type. This result disagrees with the conclusion of the previous ultrasonic study that a ferroelastic phase transition is expected.¹ The present result supports the x-ray result that KHCO_3 undergoes an antiferrodistortive phase transition.²⁻⁴

The origin of the incomplete softening of the c_{66} and the c_{22}''' modes is discussed. Hereafter, we employ the notation $F(c)$ to express the elastic stiffness constant c in the frequency dimension as

$$F(c) = \left(\frac{|q|}{2\pi} \right) \sqrt{\frac{c}{\rho}}. \quad (1)$$

Here q is the scattering vector and ρ is the density of the sample. The elastic stiffness constant of the c_{22}''' mode is expressed as

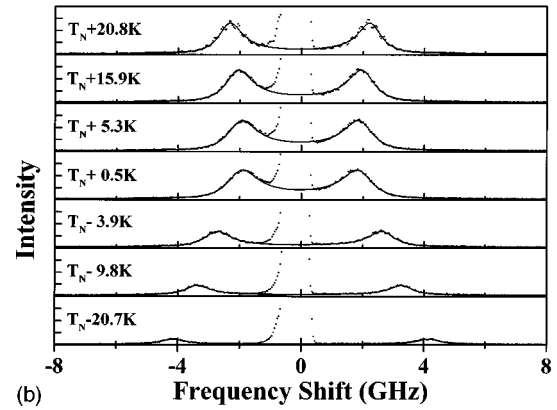
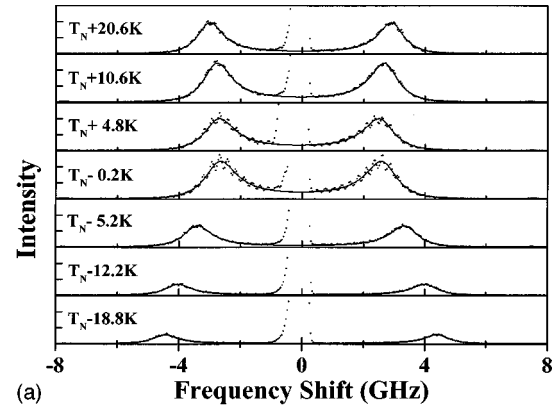


FIG. 3. The typical Brillouin scattering spectra of (a) the c_{66} and (b) the c_{22}''' modes at several temperatures near $T_N=318$ K. Thin curved lines indicate the result of the least squares fit of a damped-harmonic oscillator function.

$$c_{22}''' = \frac{c_{66} + c_{44} - \sqrt{(c_{66} - c_{44})^2 + 4c_{46}^2}}{2}. \quad (2)$$

By the use of Eqs. (1) and (2), $F(c_{46})$ can be evaluated directly from the frequency shift data of the observed c_{22}''' , c_{44} , and c_{66} modes without the knowledge of $|q|$ and ρ . Here we assume that there is no anisotropy in the refractive index

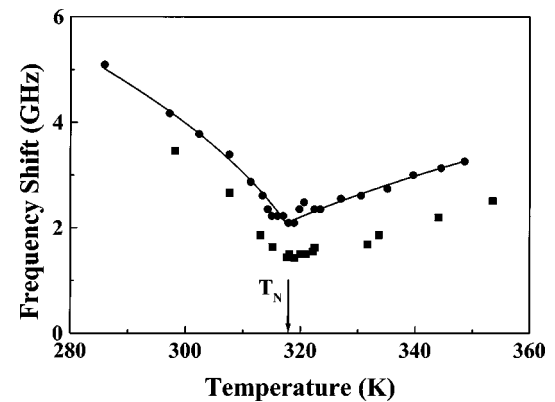


FIG. 4. The temperature dependence of the frequency shifts of the c_{66} (closed circles) and the c_{22}''' (closed squares) modes near $T_N=318$ K. The curved full lines indicate the result of the least squares fit of Eq. (5) to the frequency shift data of the c_{66} mode.

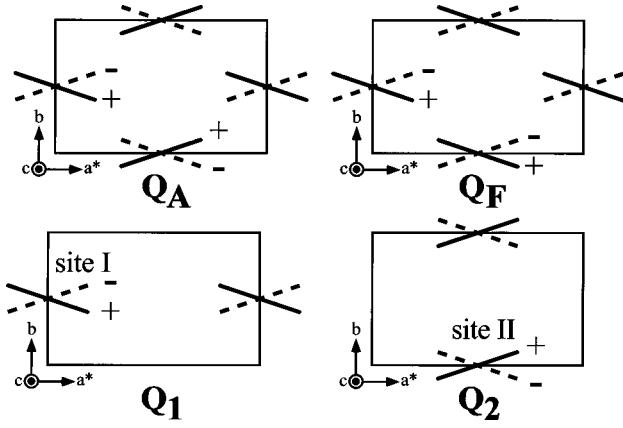


FIG. 5. The configuration of $(\text{HCO}_3)_2$ dimers (solid and dashed lines) corresponding to each of parameters Q_A , Q_F , Q_1 (at site I), and Q_2 (at site II) on the c -axis projection of the unit cell. The set of solid lines and that of dashed ones define the positive (+) and negative (-) signs of each parameter, respectively. The parameters Q_A and Q_F are related to Q_1 and Q_2 as $Q_A = (Q_1 + Q_2)$ and $Q_F = (Q_1 - Q_2)$.

n , though $|\mathbf{q}|$ directly depends on n . The temperature dependence of $F(c_{46})$ is added in Fig. 2. Since the frequency shift of the c_{44} mode and $F(c_{46})$ are almost independent of temperature as seen in Fig. 2, one can deduce that the softening behavior of the c_{22}'' mode is caused mainly by that of the c_{66} mode. It is obvious that this deduction is not affected at all by the above assumption.

In order to explain the incomplete softening of the c_{66} mode, we can employ the free energy G expanded with the elastic strain x_i (i runs from 1 to 6) and with the parameters Q_A and Q_F . Here Q_A and Q_F express the antiferrodistortive and ferrodistortive orders of the dimers, respectively, as shown in the upper half of Fig. 5. The parameter Q_A should be the order parameter describing the antiferrodistortive phase transition of KHCO_3 . It corresponds to the Brillouin zone boundary mode, the wave vector \mathbf{k} of which is equal to the unit vector \mathbf{a}^* of the reciprocal lattice in phase I.² This boundary mode belongs to the irreducible representation $\hat{\tau}_3$ of the space group $C2/m$ at $\mathbf{k} = \mathbf{a}^*$, where $\hat{\tau}_3$ is the notation given in Kovalev's Table T4.⁵ The parameter Q_A corresponds to the Brillouin zone center mode belonging to the irreducible representation A_g of the point group $2/m$ in phase II. On the other hand, the parameter Q_F is related to the Brillouin zone center mode belonging to the irreducible representation B_g of the point group $2/m$ in both phases I and II. The introduction of Q_F into the free energy G is essential for the explanation of the incomplete softening of the c_{66} mode.⁶ Because Q_A and Q_F are symmetrically nonequivalent, the temperature dependence of the coefficients of the Q_A^2 and Q_F^2 terms is not evident. The patterns Q_A and Q_F can be generated by new parameters Q_1 and Q_2 : $Q_1 = (Q_A + Q_F)/2$ and $Q_2 = (Q_A - Q_F)/2$. The new parameters are symmetrically equivalent and independent in phase I as shown in the lower half of Fig. 5. The free energy G in phase I is expanded by Q_1 , Q_2 , and x_i according to the symmetry of the space group $C2/m$ as

$$G = \frac{1}{2}A(Q_1^2 + Q_2^2) + \frac{1}{4}B(Q_1^4 + Q_2^4) + \xi Q_1 Q_2 + \eta(Q_1 - Q_2)x_6 + \frac{1}{2}c_{66}^0 x_6^2. \quad (3)$$

Here A , B , ξ , and η are the expansion coefficients and c_{66}^0 is the elastic stiffness constant at constant Q_1 and Q_2 .⁷ In this equation, only the lowest order of couplings among Q_1 , Q_2 , and x_i are considered. Another lowest coupling term $(Q_1 - Q_2)x_4$ can be included in Eq. (3), but it is neglected because the effect is estimated to be small by the observation of the c_{44} mode as shown in Fig. 2. To discuss the temperature dependence of c_{66} , we assume that the coefficient A has a linear temperature T dependence as $A = \alpha(T - T_0)$ with positive constants α and T_0 . The bilinear couplings among Q_1 , Q_2 , and x_i ($i = 1, 2, 3$, and 5) do not appear in Eq. (3) due to the crystal symmetry. This explains the present experimental fact that the c_{11} , c_{22} , c_{33} , and c_{55} modes do not show any anomalous behaviors as seen in Fig. 2.

Three sets [cases (I), (II), and (III)] of the stable solutions of $\langle Q_1 \rangle$, $\langle Q_2 \rangle$, and $\langle x_6 \rangle$ are obtained from the equilibrium condition $\partial G / \partial Q_1 = \partial G / \partial Q_2 = \partial G / \partial x_6 = 0$ and from the minimization of the free energy as follows.

Case (I): $\langle Q_1 \rangle = \langle Q_2 \rangle = \langle x_6 \rangle = 0$. This case corresponds to phase I.

Case (II): $\langle Q_1 \rangle = \langle Q_2 \rangle \equiv Q$ and $\langle x_6 \rangle = 0$, where $Q^2 = -(A + \xi)/B$. This case corresponds to phase II. The minimum of G is calculated as $G = -(T_N - T)^2 / 2B$. The phase transition temperature T_N is defined as $T_N = T_0 - \xi / \alpha$.

Case (III): $\langle Q_1 \rangle = -\langle Q_2 \rangle \equiv Q$ and $\langle x_6 \rangle = -2\eta Q / c_{66}^0 \equiv x_{6s}$, where $Q^2 = -(A - \xi - 2\eta^2 / c_{66}^0) / B$. The dimers align with ferrodistortive configuration Q_F as shown in Fig. 5 and the space group should become triclinic $P\bar{1}$. The minimum of G is calculated as $G = -(T_C - T)^2 / 2B$. The phase transition temperature T_C is defined as $T_C = T_0 + (\xi + 2\eta^2 / c_{66}^0) / \alpha$. The spontaneous strain x_{6s} appears and the c_{66} mode takes zero frequency value at T_C . Since the antiferrodistortive phase transition in KHCO_3 is concluded in the present study, case (III) must be omitted. To be consistent with this result, the value of G in case (III) should always be larger than the value of G in case (II). This gives the relation $T_C < T_N$, which is equivalent to the condition

$$\xi + \frac{\eta^2}{c_{66}^0} < 0. \quad (4)$$

The temperature dependence of the elastic stiffness c_{66} is given finally as

$$c_{66} = c_{66}^0 - \frac{2\eta^2}{\alpha(T - T_N) - 2\xi}, \quad \text{for } T \geq T_N, \\ = c_{66}^0 - \frac{2\eta^2}{2\alpha(T_N - T) - 2\xi}, \quad \text{for } T \leq T_N. \quad (5)$$

The incomplete softening behavior observed in the present study is explained well by Eqs. (4) and (5). Especially, these equations assure that c_{66} has a positive value of $c_{66}^0 + \eta^2 / \xi$ even at $T = T_N$. The frequency $F(c_{66}^0 + \eta^2 / \xi)$ is determined

experimentally to be 2.1 GHz at $T=T_N$. Expanding Eq. (5) in terms of $(T-T_N)$ and approximating it by the first term, it is rewritten in the unit of frequency and is used for the least squares fit to the frequency shift data of the c_{66} mode. The fit is done simultaneously in both phases I and II under the assumption of the linear temperature dependence of c_{66}^0 . The successful result is obtained and is drawn by the curved full lines in Fig. 4. There are two independent fitting parameters which correspond to $\alpha\eta^2/\xi^2$ and to the temperature gradient of c_{66}^0 through Eq. (1). The value of the parameter corresponding to $\alpha\eta^2/\xi^2$ and that to the temperature gradient of c_{66}^0 are determined to be 0.58 ± 0.02 GHz²/K and -0.08 ± 0.01 GHz²/K, respectively.

In summary, we report here a Brillouin scattering study of KHCO_3 . It is elucidated by a careful experiment that the c_{66} and the c_{22}''' modes never take zero frequency values even at T_N . This supports the result of x-ray study which suggests an antiferrodistortive phase transition of KHCO_3 . By the present result, we solved the early inconsistency between the ultrasonic and x-ray studies. The softening behavior of the c_{22}''' mode is explained by the temperature dependence of the c_{66} mode. The incomplete softening of the c_{66} mode is discussed phenomenologically and explained well quantitatively.

The present study was supported in part by Grant-in-Aid for Scientific Research (A) from the Ministry of Education, Science and Culture of Japan, No. 06402009.

-
- ¹S. Haussühl, *Solid State Commun.* **57**, 643 (1986).
²S. Kashida and K. Yamamoto, *J. Solid State Chem.* **86**, 180 (1990).
³I. Nitta, Y. Tomiie, and C. H. Koo, *Acta Crystallogr.* **5**, 292 (1952).
⁴J. O. Thomas, R. Tellgren, and I. Olovsson, *Acta Crystallogr. Sect. B* **30**, 1155 (1974).
⁵O. V. Kovalev, *Irreducible Representations of the Space Groups* (Gordon and Breach, New York, 1965).
⁶If the free energy G is expanded in powers of Q_A and the elastic strains x_i as

$$G = \frac{1}{2}aQ_A^2 + \frac{1}{4}bQ_A^4 + \sum_{i=1,2,3,5} \eta_i Q_A^2 x_i + \frac{1}{2} \sum_{(i,j)} c_{ij}^0 x_i x_j,$$

one cannot explain the anomalous behavior of the c_{66} mode. Even if higher order terms related to the elastic strain x_6 are

added to G , the softening behavior of the c_{66} mode above T_N cannot be explained. These results are caused by the neglect of Q_F .

⁷One can express the free energy G with Q_F and Q_A as

$$G = \frac{1}{2} \left(\frac{A+\xi}{2} \right) Q_A^2 + \frac{1}{4} \left(\frac{B}{8} \right) Q_A^4 + \frac{1}{2} \left(\frac{A-\xi}{2} \right) Q_F^2 + \frac{1}{4} \left(\frac{B}{8} \right) Q_F^4 + \frac{1}{4} \left(\frac{3B}{4} \right) Q_A^2 Q_F^2 + \eta Q_F x_6 + \frac{1}{2} c_{66}^0 x_6^2.$$

The distinct feature is that both coefficients of Q_A^2 and Q_F^2 depend on temperature through $A = \alpha(T-T_0)$. It is apparent that Q_F causes the c_{66} mode softening through the bilinear coupling $\eta Q_F x_6$. This form of G is obtained from Eq. (3) by the use of relations $Q_1 = (Q_F + Q_A)/2$ and $Q_2 = (Q_A - Q_F)/2$.